SMART SPRING CONCEPT FOR HELICOPTER VIBRATION AND NOISE CONTROL

David G. Zimcik, Chen Yong, Viresh K. Wickramasinghe and Fred Nitzsche*
(Institute of Aerospace Research, National Research Council, Ottawa, Canada)
(*Department of Mechanical and Aerospace Engineering, Carleton University, Ottawa, Canada)

Keywords: *helicopter vibration, structural dynamics, adaptive control*

Abstract

Significant structural vibration is a notable and undesirable characteristic in helicopter flight that leads to structural fatigue, poor ride quality for passengers and high acoustic signature for the vehicle. Previous Individual Blade Control (IBC) techniques to reduce these effects have been hindered by electromechanical limitations of piezoelectric actuators. The Smart Spring is an unique IBC approach for rotor vibration suppression that adaptively alters the "structural impedance" at the blade root. An adaptive notch Individual Blade Control algorithm to suppress the vibration in frequency domain has been developed and implemented based on a mathematical model to predict frequency response. Reference signal synthesis techniques were used to automatically track the shifts in the fundamental vibratory frequency due to variations in flight conditions. Closed-loop tests performed on the proof-of-concept hardware achieved significant vibration suppression at harmonic peaks as well as the broadband reduction in vibration. Investigation verified the capability of the Smart Spring to suppress multiple harmonic components in rotor vibration through active impedance control.

1 Introduction

Helicopter rotors operate in a highly complex, unsteady aerodynamic environment caused by cyclic variation of centrifugal and aerodynamic loads on the blades. Significant structural vibration due to unsteady aerodynamics caused by blade vortex interaction (BVI) and dynamic blade stall is a notable and undesirable characteristic of helicopter flight [1].

The most important sources that contribute to the vibration in helicopter airframe, are the rotor hub reactions induced by the inertial and aerodynamic loads acting on the blades. Most of the aerodynamic vibratory loads produced by the rotator system cancel at the hub, except for their PN/rev harmonics, where P is an arbitrary integer number, and N is the number of blades [2]. Due to the inherent coupling between the rotor system and the airframe, vibratory hub loads are transferred throughout the helicopter structure. This structural vibration contributes to poor ride quality for passengers, fatigue of expensive structural components, and high acoustic signature for the vehicle.

Increasing efforts have been devoted to implement active control techniques to significantly reduce vibration. These active approaches promise vibration suppression in a broadband of frequencies unlike the passive techniques that are typically capable of controlling vibration only at a specific frequency.

Individual Blade Control (IBC) is one of the active control techniques currently under development that offers suppression of discrete and broadband vibration. IBC places actuators on the blade or the swash plate to control each blade independently and simultaneously. IBC can be more effective when comprised of several subsystems, each controlling a specific mode that contributes significantly to the vibration [3]. Implementing a synthesized control system minimizes the vibration modes on each blade to reduce the magnitude of the hub reactions in the rotating frame, thereby suppressing the fuselage vibration.

There are a number of conventional IBC implementations, but most have serious

shortcomings [4]. Capabilities of conventional servo-hydraulic actuator systems are limited due to system complexity, slow response, etc. Recent advances in active material actuators that offer direct conversion of electrical energy to produce high frequency mechanical motion provide a potential to overcome these limitations. Furthermore, these systems have fewer parts compared to conventional systems, which would simplify the system.

IBC using active material actuators for rotor vibration suppression has been implemented using two distinct actuation concepts, namely, discrete and integral. The discrete actuation concept employs an actuator imbedded in the blade to control a trailing edge servo-flap [5, 6]. Unfortunately, a fundamental problem with these approaches is the limited displacement capability of piezoelectric actuators. Robust and compact displacement amplification devices are necessary to obtain the required flap deflection under the extreme aerodynamic environment of a rotor blade.

In the integral actuation concept, the actuator system is either embedded or bonded to the skin along the blade span to obtain a smooth continuous structural deformation [7,8]. The drawback with this approach is the requirement of very high voltages to induce sufficient actuation from the actuators. A 3000Vpp driving voltage cycle is required to generate the required blade twist for rotor vibration suppression [9].

It is important to note that all of the above IBC approaches attempted to actively alter the time varying aerodynamic loads on the blade. Successful implementation of these approaches has been hindered by the electromechanical performance limitations of the active material actuators, specifically the piezoelectric actuators. Restricted deformation capabilities of these actuators required complex displacement amplification mechanisms or application of extremely high voltages in order to achieve the required vibration suppression performance.

The Smart Spring provides an unique approach for IBC that overcomes these difficulties. This paper describes the concept of the Smart Spring for helicopter rotor vibration suppression. A mathematical model was developed for the non-linear dynamic characteristics of the Smart Spring and to provide a basis for active impedance control to suppress the multiple harmonic components in the blade vibration. Based on this model, an adaptive notch algorithm was developed for the higher harmonic vibration suppression applications. Proof-of-concept hardware performance test results are presented.

2 Smart Spring Concepts for Active Vibration Control

To achieve the goal of rotor vibration suppression using IBC, it is possible to alter either the time varying aerodynamic loads on each blade, or the structural stiffness of the blades in response to the blade vibration [3]. In contrast to direct control of aerodynamic loads through a trailing edge flaps or integral blade twist, Smart Spring is an unique approach to suppress the rotor vibration by adaptively varying the structural impedance, which is comprised of dynamic stiffness and effective mass in the complex form. The Smart Spring overcomes many limitations of other IBC approaches that have been implemented using piezoceramic actuators.

2.1 Smart Spring Concept

The Smart Spring is a patented* concept based on an active stiffness device that adaptively varies the structural impedance to suppress vibration [10]. The basic Smart Spring concept can be illustrated as two springs in parallel with spring constants k_1 and k_2 as shown in Fig. 1. The spring with constant stiffness k_2, provides the primary stiffness to the structure and the properties of the active spring k_1 is dynamically varied in an adaptive manner. An active material actuator attached to the active spring facilitates this process. The actuator is inserted in a structural sleeve to engage the structure in the direction perpendicular to the vibration by actuating against the sleeve. The variable

* US # 5,973,440, 1999 and EU # EP-996570-B1, 2001

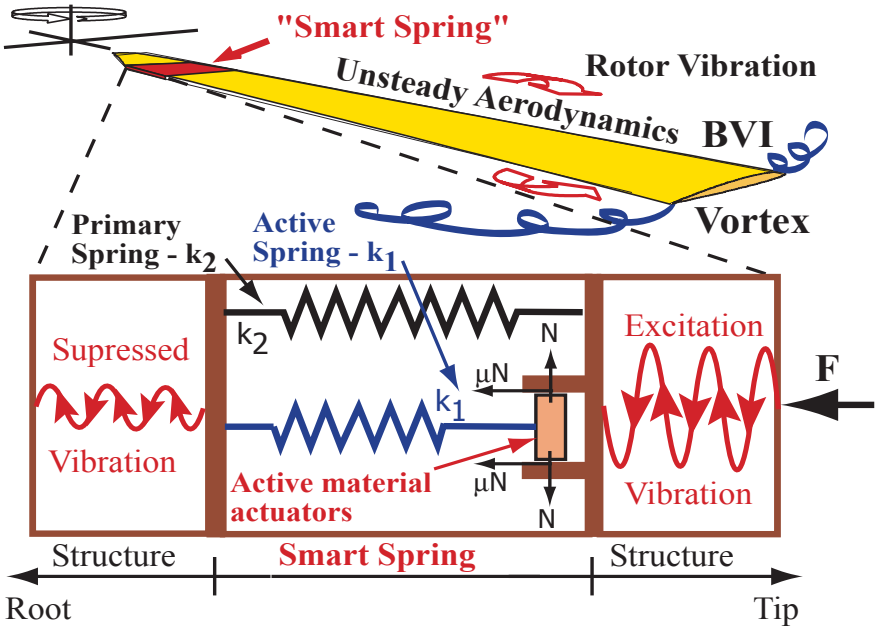

Fig. 1: Schematic of the Smart Spring Concept

frictional force μN, produced at the interface of the actuator due to the normal action force N, is used to engage the active spring to the structure. The controllable variation in stiffness as well as mass introduced by k_1 enables active impedance control of the structure to suppress the vibration transferred through the Smart Spring within a broadband of frequencies. Moreover, this is facilitated with only a small deformation of the actuators.

A Smart Spring is incorporated into each blade control individual blade independently in the rotating frame in order to achieve a global reduction in the vibration at the fuselage. The Smart Spring device is placed near the blade root to dynamically alter the response of the blade to control the vibratory reaction forces in the hub [11]. The root is the optimum location for a Smart Spring device to dampen blade vibration because the structural loads are the highest and the damper has the greatest effect. The adaptive nature of the Smart Spring controller is able to track the changes in the fundamental vibratory frequencies and operate the Smart Spring to have the greatest vibration suppression performance. This is a vast improvement over passive vibration suppression techniques that may only dampen rotor vibration at a specific frequency.

2.2 Smart Spring Mathematical Model for Harmonic Control

The Smart Spring is mathematically modeled as two springs, k_1 and k_2, within the same structural configuration as shown in Fig. 1. The external force F applied to one side of the structure provides the vibratory excitation. When the actuator is turned "off," the vibratory forces are transmitted only through the constant stiffness spring designated by k_2. When the actuator is turned "on," the frictional force μN engages the active spring to carry the vibratory loads through the Smart Spring. Controllable engagement of the active spring enables the introduction of active impedance control to filter the vibratory forces before transferring them to the opposite side of the structure.

When motion is involved, the friction coefficient μ is expected to vary from its dynamic, lower limit, μ_k to its static, higher limit, μ_s. The actual process may be complicated, however, as a first approximation, one can assume that a process where dry friction or "structural damping" is present. This constant contact with the structural sleeve is beneficial to the stability of control process because it is preferable to have a smooth, rather than abrupt, variation on the stiffness. In the later case, an on-off type of control would be

present. Such a system would excite many structural modes during the transients, degrading the robustness of the system. Therefore, if the external force F is harmonic on the frequency and assuming that the total inertia of the system is represented by m, the equation of motion on the horizontal displacement x is given by:

$$m\ddot{x} + k(t)x = Fe^{j\omega t} \tag{1}$$

In the above equation, the magnitude of the stiffness parameter varies between the two theoretical limits, i.e.:

$$k_2 \le |k(t)| \le k_1 + k_2 \tag{2}$$

If the control law is harmonic and the variation on the stiffness parameter is proportional to the electrical stimulus, which is externally applied to the piezoelectric stack, it can be expanded into a complex Fourier series:

$$k(t) = \sum_{r=-\infty}^{r=\infty} k_r e^{ir\Omega t} \tag{3}$$

Where $\Omega = 2\pi/T$, T is the period associated with the cycle of actuation and the coefficient can be expressed as:

$$k_r = \frac{1}{T}\int_0^T k(t)e^{-ir\Omega t}dt \qquad r = 1,2,\cdots,\infty \tag{4}$$

Assuming that the solution is harmonic on the multiples of the exciting frequency,

$$x(t) = \sum_{r=-\infty}^{\infty} x_r e^{ir\omega t} \tag{5}$$

Where the coefficients associated with the negative harmonics are simply the complex conjugates of their positive harmonic counterparts ($x_{-r} = x_r^*$). Assuming that the control law is composed of only one harmonic and that the mean value of the stiffness coefficient is k_0:

$$k(t) = k_1^* e^{-i\Omega t} + k_0 + k_1 e^{i\Omega t} \tag{6}$$

Since $k_{-1} = k_1^*$, substituting *k(t)* into (1) and (5), the following is obtained:

$$\sum_{r=-\infty}^{\infty}\left[\left(-mr^2\omega^2 + k_0\right)e^{ir\omega t} + k_1^* e^{i(r\omega-\Omega)t} + k_1 e^{i(r\omega+\Omega)t}\right]x_r = Fe^{i\omega t} \tag{7}$$

Assuming that the control frequency is equal to the exciting frequency, $\omega = \Omega$ (this is actually the case for the most applications involving helicopter IBC), one obtains:

$$\sum_{r=-\infty}^{\infty}\left[\left(-mr^2\omega^2 + k_0\right)e^{ir\omega t} + k_1^* e^{i(r-1)\omega t} + k_1 e^{i(r+1)\omega t}\right]x_r = Fe^{i\omega t} \tag{8}$$

A transformation in the dummy indices in the summation is performed next. In equation (8), the two main terms involving frequency shifts are rewritten as:

$$x(t) = \sum_{r=-\infty}^{\infty} x_r e^{i(r-1)\omega t} = \sum_{r+1=-\infty}^{r+1=\infty} x_{r+1} e^{ir\omega t} \tag{9}$$

$$x(t) = \sum_{r=-\infty}^{\infty} x_r e^{i(r+1)\omega t} = \sum_{r-1=-\infty}^{r-1=\infty} x_{r-1} e^{ir\omega t} \tag{10}$$

Replacing the corresponding terms in (8), this equation now becomes:

$$\sum_{r=-\infty}^{\infty}\left[\left(-mr^2\omega^2 + k_0\right)x_r + k_1^* x_{r+1} + k_1 x_{r-1}\right]e^{ir\omega t} = Fe^{-i\omega t} + Fe^{i\omega t} \tag{11}$$

Where the exciting force is extended to include the mirror image and negative harmonic to keep the symmetry of the series. Notice the $F_{-1} = F_1^* = F$ since F is a real quantity. Applying harmonic balance to equation (11), the following set of tri-diagonal equations on the complex coefficients of the frequency response is obtained:

$$\begin{bmatrix} \ddots & \ddots & & & & & & \\ \ddots & -4m\omega^2 + k_0 & k_1^* & & & & & \\ & k_1 & -m\omega^2 + k_0 & k_1^* & & & & \\ & & k_1 & k_0 & k_1^* & & & \\ & & & k_1 & -m\omega^2 + k_0 & k_1^* & & \\ & & & & k_2 & -4m\omega^2 + k_0 & \ddots & \\ & & & & & \ddots & \ddots & \end{bmatrix} \begin{Bmatrix} \vdots \\ x_{-2} \\ x_{-1} \\ x_0 \\ x_1 \\ x_2 \\ \vdots \end{Bmatrix} = \begin{Bmatrix} \vdots \\ 0 \\ F \\ 0 \\ F \\ 0 \\ \vdots \end{Bmatrix} \tag{12}$$

The harmonic coefficients with indices –1, 0 and 1, can be expressed respectively as:

$$\begin{aligned} &\vdots \\ &x_{-1} = x_1^* \\ &x_0 = \frac{-(k_1 + k_1^*)}{(-m\omega^2 + k_0)k_0 - 2k_1 k_1^*} F \\ &x_1 = \frac{(-m\omega^2 + k_0)k_0 + k_1^2 - k_1 k_1^*}{(-m\omega^2 + k_0)[(-m\omega^2 + k_0)k_0 - 2k_1 k_1^*]} \\ &\vdots \end{aligned} \tag{13}$$

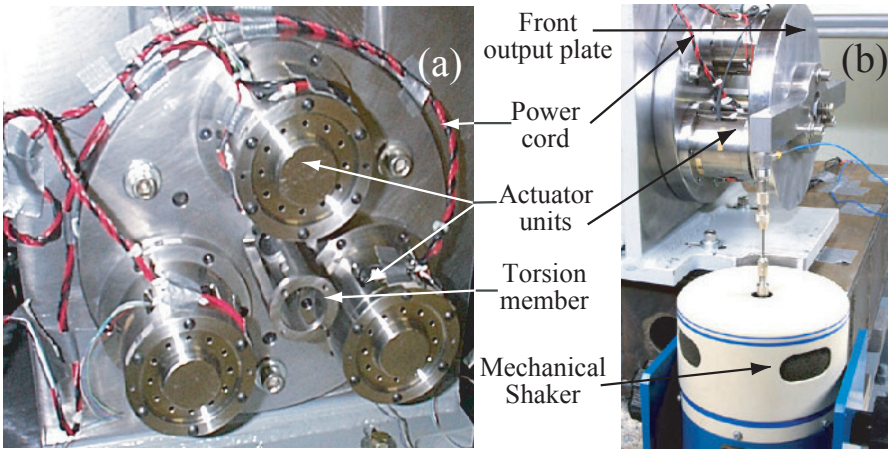

Fig. 2: Proof-of-concept hardware

Hence, a discrete complex frequency response, characterized by magnitude and phase shift, is obtained. As a first approximation according to equation (13), it can be deduced that the introduction of the active spring, or "impedance control," causes redistribution of the dynamic response spectrum of the structure.

This analysis shows the integration of the Smart Spring at the root of the blade introduces a non-linear variation in structural impedance that attenuates reaction forces at the hub. Furthermore, single harmonic control of the Smart Spring leads to the changes in the response of multiple harmonic components. It suggests that by actively controlling the Smart Spring, according to an appropriate harmonic control law, multiple harmonic components in the root response can be changed at the same time.

3 Proof-of-Concept Hardware Developments

Proof-of-concept hardware was fabricated to verify the Smart Spring concept for active vibration control. The hardware was designed to suppress torsional vibration through adaptive structural control.

The Smart Spring proof-of-concept hardware design included three "actuator units" to apply a balanced load to an output plate. Interaction between the actuator units and the output plate generates the frictional forces necessary to engage the actuator units as active members to vary the structural impedance of the device. The primary stiffness of the device was tailored through the design of the central torsion member to match a typical blade torsional stiffness. The proof-of-concept hardware without the front output plate is shown in Fig. 2a and the complete proof-of-concept hardware with the front output plate attached to the mechanical shaker* is shown in Fig. 2b.

A mechanical shaker simulated the excitation vibration forces from rotor blade on the Smart Spring device. A load transducer† installed on the shaker attachment stinger measured the vibratory forces from the shaker. On the opposite side from the shaker on the output plate, a displacement probe‡ measured the vibratory displacement of the output plate.

Stacked piezoelectric actuators§ that could provide greater than 3388N of blocked-force at the maximum input voltage of +100V were chosen for the actuator unit design. A total of three actuators were mechanically arranged in series to improve the overall deflection of the actuator unit while the actuators were electrically connected in parallel to maintain force and voltage requirements. A miniature ring load cell†† was incorporated into each actuator assembly to measure the force generated by the unit on the front output plate.

The actuator units could be preloaded using a central bolt through the torsion member

* LMT-100 Thruster, Ling Electronics Inc., Anaheim, CA.
† 208B02, PCB Piezotronics, Depew, NY.
‡ S-DVRT-24, MicroStrain Inc., Burlington, VT.
§ TS18-H5-202, Piezo Systems Inc., Cambridge, MA.
** DFS, National Research Council Canada, Ottawa, ON.
†† ELW-D3, Entran Sensors and Electronics, Fairfield, NJ.

to investigate the effect on impedance augmentation performance of the Smart Spring. A challenge for this Smart Spring design was to keep the displacement of the actuators as low as possible to maximize the force generated by the actuator unit. Furthermore, the actuator unit surface and output plate surface must maintain a high coefficient of friction for effective engagement of the actuator units while remaining wear resistant.

Initial tests on the Smart Spring proof-of-concept hardware were conducted to evaluate the predicted performance of each individual component, particularly the actuator units. These component level verification test results confirmed that the actuation forces generated by each unit effected impedance augmentation using this Smart Spring hardware.

4 Adaptive Controller Developments

As illustrated by the mathematical model, the Smart Spring provides an approach to suppress multiple harmonic components in blade vibration by actively controlling the piezoceramic actuators. Because most of helicopter vibration comes from only a few higher harmonic components, it is possible to control the Smart Spring in a related frequency domain to achieve significant suppression in structural vibration.

4.1 Open Loop Strategy

In the initial phase of the controller development, an open loop control algorithm was implemented which achieved significant suppression in vibratory displacement when the Smart Spring actuators were activated ~90° out of phase from the excitation vibration. This suggested that a closed loop control algorithm could greatly improve the vibration suppression performance of the Smart Spring.

4.2 Closed-loop Strategy

The Smart Spring device was predicted to exhibit non-linear dynamic characteristics due to the operation of piezoelectric actuators and the frictional forces between the mating surfaces. Therefore, an adaptive notch controller based on a Filtered-U recursive LMS algorithm was developed as the closed-loop control strategy to suppress the harmonic components in blade vibration.

4.2.1 Adaptive Notch Controller

In the current model, only torsional vibration is controlled using the Smart Spring proof-of-concept hardware. Since all of the actuator units were connected in parallel to one independent control channel, a SISO adaptive controller was sufficient for this task. The structure of a SISO adaptive notch controller with on-line identification of the secondary path and a reference signal synthesizer is shown in Fig. 3. A MIMO controller could be developed for the present system to satisfy different configurations of actuators for bending or bending-torsion combined vibration control.

The adaptive notch controller can be described in the discrete time domain [12]. The aerodynamic load g(n) is transferred from the blade to the rotor hub according to the transfer function matrix Gp. This represented the primary path, producing a disturbance vibration vector represented by the signal d(n). The secondary path Gs represented the additional impedance provided by the active spring. The actuator input and vibration output were described as u(n) and y(n), respectively. The vibration of the blade measured by the displacement probe was denoted by e(n). A Infinite Impulse Response (IIR) controller, which was adapted by the output signal of status observer, was used to filter the reference input signal x(n) to produce the control signal, which was then amplified to apply the required voltage to the actuators. The overall objective of the adaptive notch controller was to minimize the RMS value of the blade torsional vibration and the hub reaction forces.

4.2.2 Algorithm Simplifications

A secondary path on-line identification loop to account for time-variable characteristics is also shown in Fig. 3. This requires the identification process to occur in parallel with the control

[*] LE150/200, Piezomechanik GmbH, Munich, Germany.

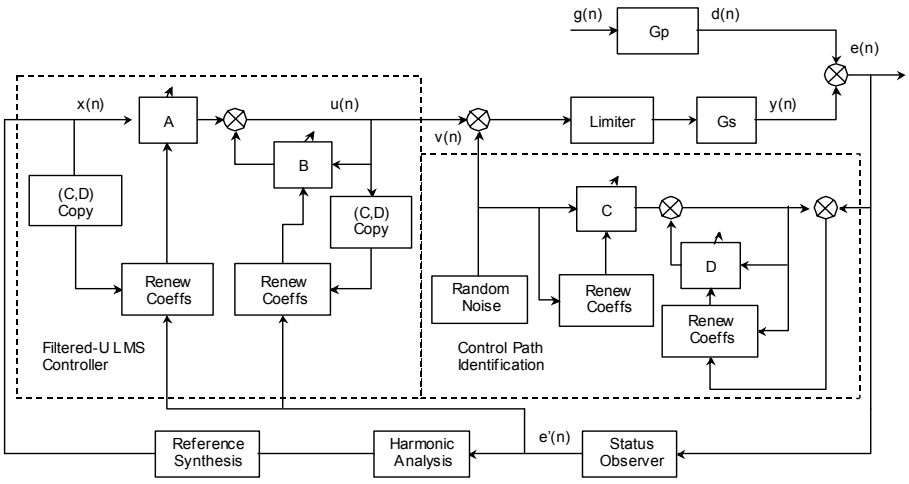

Fig. 3: Structure of adaptive notch controller

process. The performance of such a controller is sensitive to the strength of the training random signal, which must be high for good system identification. However, the training signal strength must be as low as possible to implement effective control. These contradicting requirements for the training signal strength for on-line identification have been proven to be difficult to implement. Furthermore, the computational speed requirement for real-time system identification and control simultaneously is high, especially for the case of high frequency control.

Assuming slow variation of plant model coefficients and zero initial conditions, off-line identification was used for the secondary path identification. However, real-time system identification was recognized as a requirement to be implemented during wind tunnel aerodynamic loading tests.

4.2.3 Reference Signal Synthesis

The reference signal is a very important factor in feed-forward adaptive controllers. One approach is to measure the primary disturbance using a suitable reference sensor and use the output directly as the required reference. This technique is effective for both broadband (random) and narrowband (periodic) disturbances. However, one limitation is that a feedback loop must be introduced to the adaptive controller and could affect system stability.

A digital wave synthesis technique was used to overcome the difficulty of providing a stable reference signal. An advantage of the digital wave synthesis is the selectivity of frequency band, which is important for higher harmonic control problems associated with helicopter vibration. Also, it is only necessary to model the secondary path transfer function over the selected frequency band, substantially lowering the order of the filters required to improve the efficiency of the control algorithm.

Because the harmonic frequencies (PN/rev) are included in the error signal e(n), both the amplitude and phase of the main components were determined using on-line FFT analysis. Assuming the magnitude and phase of each component in the hub reaction are A_m and ϕ_m, and the interval sampling time was represented by T, the reference signal was synthesized as a linear combination of sinusoids:

$$x(n) = \sum_{m=1}^{M} A_m \sin(\omega_m nT + \phi_m) \qquad (14)$$

where M is the number of harmonic components to be suppressed. As discussed, only the first few main harmonic components contribute to vibration in helicopters, and these can be determined from the response spectrum. The fundamental vibration frequencies were determined and updated on-line to track the rotor speed changes due to variation in projected flight conditions.

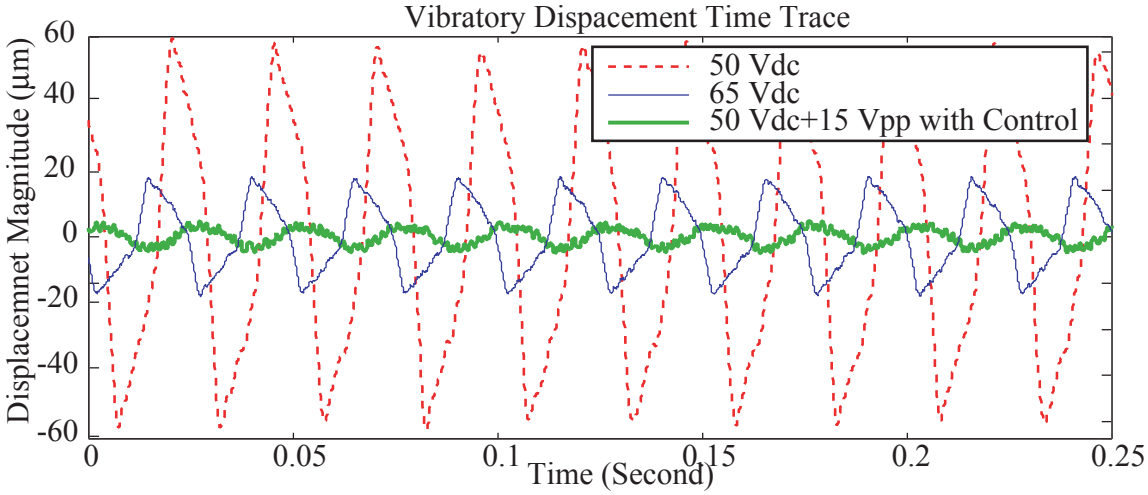

Fig. 4: Comparison of vibratory displacement

4.2.4 Algorithm DSP Implementations

The adaptive notch controller defined above was implemented on a DSP board* equipped with a Texas Instruments TMS320C40 processor. Input / Output (IO) operation was provided on a separate subsystem, PCI16O8, which is a 12-bit data acquisition and control board with 16 channels analog input and 8 channels analog output. Communication between the DSP and the IO board was achieved via a 16-bit interface. On-board third-order Butterworth anti-alias low-pass filters were used for all input and output channels. Initialization and data transferring between the host PC and the DSP were provided by a 32-bit DSPLINK interface.

The adaptive notch algorithm was programmed on the DSP platform using C and Assembler language mixed code. This allowed the use of a number of low-level programming techniques such as parallel instructions and the circular addressing mode for the implementation of the time critical aspects of the algorithm. These operations included the filter coefficients iterations, updating of the input, output vectors, filtered input and control signals. The controller output signal was amplified using the high-voltage amplifier to drive three piezoelectric actuator assemblies.

In the software implementation, the interrupt technique was used for accurate sampling of time control, with the sampling rate set to 4000 samples/second. Within the interrupt routine, the vibratory displacement of the front plate was measured as the error signal. A notch reference signal was synthesized according to the proposed algorithm, from which a control signal was calculated using a filtered-U recursive LMS algorithm. This control signal was processed by a limitation check loop before being amplified by an external amplifier. Since the FFT analysis needed a long data series and took longer to complete, it was implemented in the main program loop. Data for the FFT analysis was sampled from the error series. To improve the accuracy of frequency analysis, a lower sampling rate and a suitable length of the cycle data series had been chosen to achieve a frequency accuracy of 0.1 Hz in the harmonic component identification.

5 Test Results and Discussion

Tests were conducted on the Smart Spring proof-of-concept model at different single frequency excitations produced by the mechanical shaker. The IIR filter was implemented with 16 forward and 1 recursive coefficients with off-line identification of the secondary path.

The time traces of vibratory displacement under different test conditions are shown in Fig. 4. The excitation frequency was 40Hz and the shaker force magnitude was kept constant at 355N peak-to-peak for all test conditions. The

* QPC40B, Spectrum Signal Processing Inc. Burnaby, BC

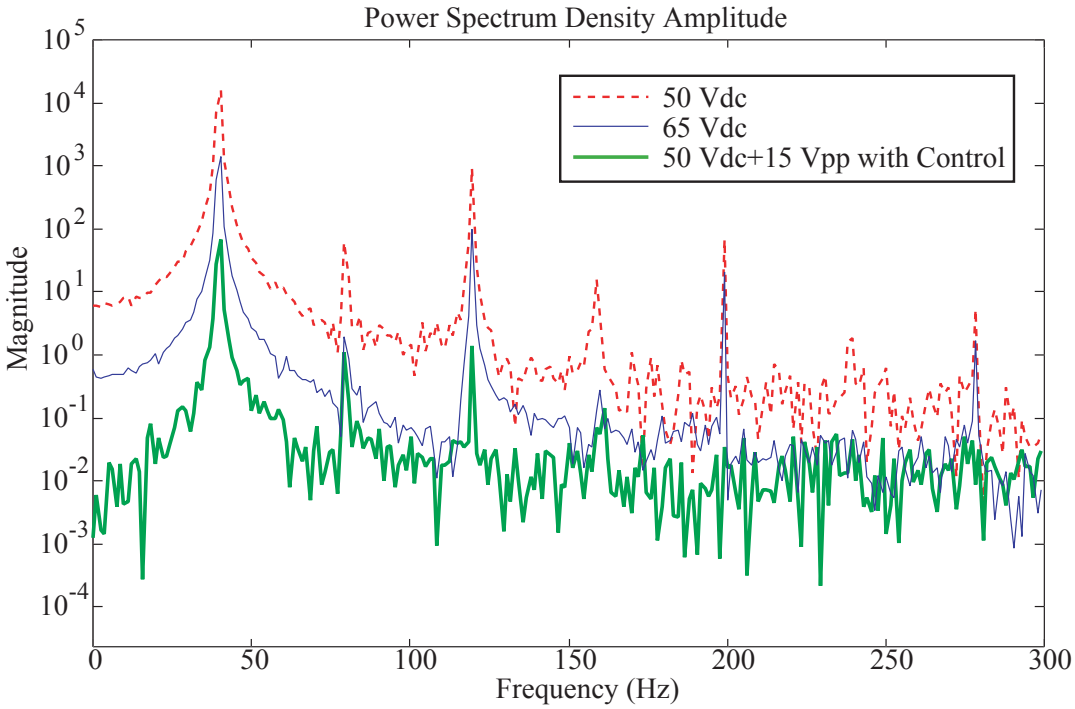

Fig. 5: PSD comparison of vibratory response

50Vdc load was the baseline operating condition of the actuators in the proof-of-concept hardware model that produced the highest vibratory displacement. Increasing the actuator voltage to 65Vdc only increased the stiffness in the Smart Spring, which in turn reduced the vibratory displacement by 5.4dB.

Table 1: Vibration suppression performance

Test Condition	50Vdc	65Vdc	50Vdc+15Vpp with Control
Displacement (RMS, μm)	36.5	10.3	2.5
Vibration Suppression (dB)		5.4	11.6

As seen from Table 1, a much higher reduction of 11.6dB in vibratory displacement was achieved by active impedance control of the Smart Spring with the use of a 50Vdc+15Vpp input voltage through the controller, compared to a static 65Vdc load. The adaptive controller used two frequencies (40Hz and 80Hz) in the reference signal synthesis to suppress the harmonic peaks. The test results showed that active impedance control through the Smart Spring not only introduced dynamic stiffness variation of the structure, but also introduced effective mass and damping in order to achieve significant suppression in vibration. The Power Spectrum Density (PSD) comparison for each test condition shown in Fig. 5 also confirms the ability of the Smart Spring to suppress vibration at multiple harmonics.

The non-linear dynamics of the Smart Spring that allows active impedance control of the blade in shown in Fig. 5. This active impedance control caused a redistribution of dynamic response spectrum at the harmonic components of the base frequency. By introducing harmonic frequencies into the synthesized reference signal of the adaptive controller, significant suppression of the main peaks (40Hz and 80Hz) was achieved. Compared to the static control scheme, imposing a pure increase in stiffness with 65Vdc, the adaptive scheme achieved significantly better reduction in overall broadband vibration and 6.2dB suppression in vibratory displacement.

It was also observed that the decrease in overall vibration was not significant even when additional frequency components were included in the synthesized reference signal. This may be the result of more harmonic components being excited by the controller output itself. As a result, the peaks of the lower frequency

components were decreased while the higher components increased slightly. Furthermore, the small convergence factor that was used to ensure the convergence of the algorithm resulted in an increase in the time required for the controller convergence. This suggested that only a few frequency components need to be included in the reference signal synthesis in order to achieve significant vibration suppression performance.

The Smart Spring proof-of-concept hardware tests described above were conducted with a shaker to simulate external aerodynamic excitation. However, extensive testing has been planned in a more representative rotor blade aerodynamic loading environment in a wind tunnel.

6 Conclusions

The Smart Spring is an unique concept for active control of helicopter rotor vibration. Rather than varying the aerodynamic driving forces, the Smart Spring alters the structural response of the blade through active impedance control at the root. This concept overcomes some of the limitations and difficulties encountered in other IBC approaches.

Both analysis and experimental results have shown that active impedance control of the structure using the Smart Spring leads to a reduction of the response spectrum in the blade that has the potential to significantly suppress multiple harmonic components in blade vibration.

The result of this investigation also demonstrated that the adaptive notch controller could track the changes in rotor speed to adaptively suppress the fundamental harmonic components of the vibration frequency by forming notches at the designated harmonics.

References

[1] Kretz M., and Larche M. Future of helicopter rotor control. *Veritical*, Vol4, pp3-22, 1980.

[2] China Aerospace Research Establishment. Helicopter aerodynamics manual. 1st Edition, China Aeronautical Industry Press, 1991

[3] Nitzsche F. and Breitbach E. J. Using adaptive structures to attenuate rotary wing aeroelastic response. *Journal of Aircraft*, Vol.31, No.5, pp1178-1188, 1994.

[4] Chen Yong, Gao Wei, TAO Baoqi and Chen Renwen. Development and testing of an adaptive rotor system based on solid actuation and non-contact signal transmission technology. *22nd Conference of International Council of Aeronautics Science*, Harrogate, UK, 2000.

[5] Prechtl, E. F. and Hall, S. R. Closed-loop vibration control experiments on a rotor with blade mounted actuation. *41st AIAA Structures, Structural Dynamics and Materials Conference*. Atlanta, USA, 2000.

[6] Straub, F. K., et al. Smart material actuated rotor technology – SMART. *41st AIAA Structures, Structural Dynamics and Materials Conference*. Atlanta, GA, 2000.

[7] Rodgers, J. P. and Hagood, N. W. Hover testing of 1/6 Mach-Scale CH-47D blade with integral twist actuation. *9th International Conference on Adaptive Structures and Technology*. Cambridge, MA, 1998.

[8] Shin, S. J., Cesnik, C. E. S. and Wilbur, M. L. Dynamic response of active twist rotor blades. *41st AIAA Structures, Structural Dynamics and Materials Conference*. Atlanta, GA, 2000.

[9] Wickramasinghe, V. K. and Hagood, N. W. Performance characterization of active fiber composite actuators for helicopter rotor blade applications. *SPIE 9th Smart Structures and Materials Symposium*. San Diego, CA, 2002.

[10] Nitzsche, F., Grewal, A. and Zimcik, D. G. "Structural Component Having Means for Actively Varying its Stiffness to Control Vibrations" US patent # 5,973,440, October 1999 and European Patent # EP-996570-B1, 2001.

[11] Nitzsche, F. Aeroelastic Analysis of a helicopter rotor blade with active impedance control at the root. *Canadian Aeronautics and Space Journal*. Vol.47, No. 1, pp7-16, 2001.

[12] Grewal, A., Zimcik, D. G. and Leigh, B. Feedforward piezoelectric structural control: An application to aircraft cabin noise reduction. *Journal of Aircraft*. Vol.38, No.1, pp164-173, 2001.